DNA Bending by Small, Mobile Multivalent Cations

Ioulia Rouzina and Victor A. Bloomfield
Department of Biochemistry, University of Minnesota, St. Paul, Minnesota 55108 USA

ABSTRACT We propose a purely electrostatic mechanism by which small, mobile, multivalent cations can induce DNA bending. A multivalent cation binds at the entrance to the B-DNA major groove, between the two phosphate strands, electrostatically repelling sodium counterions from the neighboring phosphates. The unscreened phosphates on both strands are strongly attracted to the groove-bound cation. This leads to groove closure, accompanied by DNA bending toward the cationic ligand. We explicitly treat the dynamic character of the cation-DNA interaction using an adiabatic approximation, noting that DNA bending is much slower than the diffusion of nonspecifically bound, mobile cations. We make semiquantitative estimates of the free energy components of bending—electrostatic (with a sigmoidal distance-dependent dielectric function), elastic, and entropic cation localization—and find that the equilibrium state is bent B-DNA stabilized with a self-localized cation. This is a bending polaron, formation of which should be critically dependent on the strength of electrostatic interaction and the concentration of highly mobile cations available for self-localization. We predict that the resultant bend will be large (~20–40°), smooth (because it is spread over 6 bp), and infrequent. The stability of such a bend can be variable, from transient to highly stable (static) bending, observable with standard curvature-measuring techniques. We further predict that this bending mechanism will have an unusual sequence dependence: sequences with less binding specificity will be more bent, unless the specific binding site is in the major groove.

INTRODUCTION

Deformability of double helical DNA under various solution conditions and in the presence of ligands and proteins has become a major theme of recent discussions on DNA recognition, packaging, and function. Of particular interest are changes in DNA flexibility under physiologically relevant solution conditions, i.e., mixed salts containing variable amounts of Na^+, K^+, Mg^{2+}, Ca^{2+}, and polyamine cations.

The bending and flexibility of a wormlike coil molecule such as DNA are generally characterized by its persistence length. The persistence length of high-molecular-weight DNA has been measured in the presence of low concentrations of multivalent cations by methods as diverse as linear dichroism and intrinsic viscosity (Baase et al., 1984), electrooptical techniques (Marquet and Houssier, 1988; Marquet et al., 1985, 1987; Porschke, 1984, 1986), and stretching of single DNA molecules by laser tweezers (Baumann et al., 1997; Wang et al., 1997). Substantial decreases in the persistence length of B-DNA have been observed by one or more of these techniques in the presence of multivalent cations such as Mg^{2+}, putrescine^{2+}, spermidine^{3+}, spermine^{4+}, and cobalt(III) hexaammine^{3+} ($CoHex^{3+}$). Cations with higher charge density have a stronger effect on the persistence length. This effect cannot be attributed simply to more effective Debye-Hückel-type screening of Coulombic repulsions between DNA phosphates, because the persistence length in the presence of multivalent cations drops to as little as 150 Å, much lower than the high monovalent salt limit of 500 Å (Hagerman, 1988).

Evidence of significant B-DNA bending with multivalent cations has been obtained in gel electrophoretic (Brukner et al., 1994), electrooptical (Porschke, 1986), and crystallographic (Drew and Dickerson, 1981; Goodsell et al., 1993; Kopka et al., 1983) studies. However, a variety of spectroscopic measurements such as UV (Marquet and Houssier, 1988), Raman (Duguid et al., 1993), and linear and circular dichroism (Porschke, 1986) indicate that random-sequence DNA remains essentially in the B conformation in the presence of divalent alkaline earth cations, polyamines, and $CoHex^{3+}$. Furthermore, there is a great deal of NMR evidence that these ions generally have high mobility at the DNA surface (Andreasson et al., 1993; Berggren et al., 1992; Braunlin et al., 1992; Braunlin and Xu, 1992; Wemmer et al., 1985), consistent with the sparse and variable localization of these cations in the crystal structures of DNA oligomers. Thus the data suggest that these cations are bound to B-DNA in a primarily electrostatic, nonspecific manner. The obvious question is: How do these cations with very little binding specificity induce such significant bending in B-DNA?

In this paper we suggest a purely electrostatic mechanism by which small multivalent cations can induce DNA bending. According to this mechanism, a multivalent cation binds at the entrance to the B-DNA major groove, between the two phosphate strands, electrostatically repelling sodium counterions from the neighboring phosphates. The unscreened phosphates on both strands are strongly attracted to the groove-bound cation. This leads to groove

Received for publication 13 November 1997 and in final form 17 March 1998.

Address reprint requests to Dr. Victor A. Bloomfield, Department of Biochemistry, University of Minnesota, 1479 Gortner Avenue, St. Paul, MN 55108. Tel.: 612-625-2268; Fax: 612-625-6775; E-mail: victor@maroon.tc.umn.edu.

0006-3495/98/06/3152/13 $2.00

closure, accompanied by DNA bending toward the cationic ligand.

An important point of this study is an explicit treatment of the dynamic character of the cation-DNA interaction. This issue must be confronted, because DNA bending is extremely slow on the time scale of motion of the nonspecifically bound, mobile cations. We use an adiabatic approximation to describe cation-DNA interaction in this case. We make semiquantitative estimates of the free energy components of bending—electrostatic, elastic, and entropic cation localization—and find that the equilibrium state is bent B-DNA stabilized with a self-localized cation. This is a bending polaron, the formation of which is critically dependent on the strength of electrostatic interaction and the concentration of highly mobile cations available for self-localization. The resultant bend is large ($\sim 20-40°$), smooth (because it is spread over 6 bp), and infrequent. The stability of such a bend can be variable, from transient to highly stable (static) bending, observable with standard curvature-measuring techniques. We predict that this bending mechanism has an unusual sequence dependence: sequences with less binding specificity will be more bent, unless the specific binding site is in the major groove.

This model of electrostatically induced bending differs from the other models that have been suggested in the literature: asymmetrical and phosphate neutralization (Manning et al., 1989), bending away from a neutral protein (Elcock and McCammon, 1996), or bending at the B/A/B junctions favored by a local uniform DNA phosphate charge reduction (Lebrun et al., 1997). An electrostatic mechanism of the sort we propose may underlie DNA bending by the compact cationic domains of major groove binding proteins, such as the cationic α-helices of the helix-turn-helix ZIP proteins (Fisher et al., 1992; Kerppola and Curran, 1991; Mondragon and Harrison, 1991).

PREFERENCE FOR BENDING INTO THE MAJOR GROOVE

There are a variety of reasons why cation-induced bending is usually directed into the major groove rather than the minor groove of B-DNA. The major groove has room to accommodate and close around rather bulky ligands, resulting in a significant bend. Even a relatively long chain ligand can position itself within the major groove perpendicular to the double helical axis, inducing a bending force. The internal mechanics of the B-helix family is such that the major groove does not have a low-energy option for narrowing other than by bending, whereas the minor groove can be closed without bending. Finally, as the major groove collapses, the possibility arises of extensive, and energetically favorable, hydrogen bonding between the cation and the phosphate oxygens, which in B-DNA are turned into the major groove.

In contrast, most of the nonspecifically associating multivalent cations cannot fit into the B-DNA minor groove; and those that can fit usually do not allow any further groove closure, and therefore cannot bend DNA. This is true for metal cations like Mg^{2+} and Ca^{2+}, which have an extensive hydration shell, and for the bulky $CoHex^{3+}$. Small chain cations like antibiotics or polyamines, on the other hand, fit very well into the B-DNA minor groove. Such chain cation positioning induces a force on the surrounding phosphates that tends to close the groove not by DNA bending, but rather by base pair inclination and winding. These perturbations cause straightening and rigidification of the DNA, by absorption of its intrinsic sequence-dependent curvature (Duong and Zakrzewska, 1997; Randrianarivelo et al., 1989).

Several modeling studies have described the relation of minor groove width to other conformational parameters. Zhurkin (Zhurkin et al., 1978) explored all structurally possible types of DNA double helices and showed that the family of B-DNA helices has a range of acceptable parameters, the most important of which are the twist, *x*-displacement, and inclination. Minor groove closure was invariably related to increased twisting, coupled to changes in displacement and inclination. Boutonnet et al. (1993) showed that the B-DNA minor groove width is naturally controlled by two main parameters: the base pair inclination and the *x*-displacement of the base pair along its dyad axis. Narrowing of the minor groove corresponds to increased negative inclination and the effective shift of the DNA axis into the minor groove, accompanied by moderate helix overwinding. Similar deformation results from stretching B-DNA by its 5′ ends (Lebrun and Lavery, 1996), which leads to progressively increasing negative base pair inclination accompanied by minor groove closure. The limit of extreme stretching, to about twice the B-DNA contour length, corresponds to a narrow fiber with collapsed minor and opened major grooves, and a moderate change of winding.

According to molecular modeling (Boutonnet et al., 1993), the energy required to narrow the minor groove by these deformations is larger than that required to narrow the major groove by DNA bending into it. Narrowing the minor groove by 1 Å via negative inclination costs ~ 1.5 kcal/mole of base pairs. Therefore this type of cation-induced groove deformation is usually inconsequential, occurring only when the cationic ligand has a strong preference for the minor groove.

ELECTROSTATICS OF CATION BINDING

Polyelectrolyte Aspects of Cation Binding

As a highly charged macroion, the DNA double helix in solution is always highly screened by counterions. Numerous studies, both experimental (Anderson and Record, 1990, and references therein; Braunlin et al., 1992; Braunlin and Xu, 1992; Padmanabhan et al., 1991) and theoretical (Attard et al., 1988; Fuoss et al., 1951; Gueron and Demaret, 1992; Jayaram and Beveridge, 1996; Lyubartsev and Nordenskiöld, 1995; Manning, 1978; Rouzina and Bloomfield,

1997; Schellman and Stigter, 1977; Zimm and Le Bret, 1983), have demonstrated that a large fraction of the phosphate charge is screened by counterions residing very close to the DNA surface, to an extent essentially independent of the solution ionic strength. Any attractive force in addition to electrostatics will enhance cation accumulation at the surface.

Multivalent cations are even more effective than monovalent cations in reducing the small residual charge on the scale of the Debye-Hückel screening length (Fuoss et al., 1951). This polyelectrolyte contribution becomes insignificant, however, in the presence of physiological salt concentrations, and has a modest effect, less than kT per base pair, on the energetics of DNA conformational transitions (Frank-Kamenetskii et al., 1987).

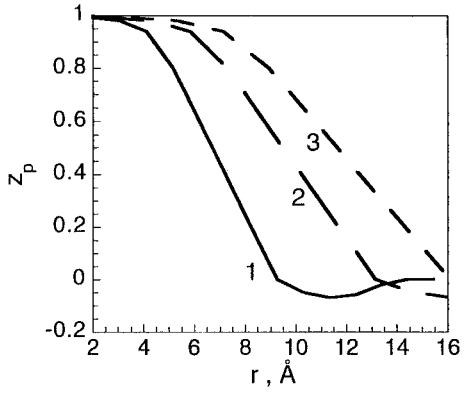

FIGURE 1 Effective charge of a DNA phosphate group, partially shielded by mobile monovalent counterions, as felt by a z-valent cation at distance r, according to Eq. 2, with dielectric function $\epsilon(r)$ given by Eq. 4. The number near each curve corresponds to the cation valence.

Electrostatic Correlation between Counterions at the Surface

The main difference between mono- and multivalent cations, for our purposes, is not that multivalent cations screen the DNA charge more effectively. Rather, it is that monovalent cations provide highly uniform screening, whereas each multivalent cation creates a local region of excess positive charge surrounded by a region of excess negative charge from the phosphates (Rouzina and Bloomfield, 1996, and references therein). With screening counterions at several molar concentration near the DNA surface, correlations between these cations can become significant. The thickness of this highly concentrated counterion layer (~1 Å) is much smaller than the radius of curvature of the DNA. It is also much smaller than the average distance between neutralizing counterions along the DNA surface $a_z = (ze/\sigma)^{1/2}$, where σ is the average polyion surface charge density. For B-DNA with an average surface charge density of one electron charge per 106 Å^2, a_z = 10.3, 14.6, and 17.9 Å for z = 1, 2, and 3, respectively. Thus the counterion correlation has a well-defined two-dimensional (2-D) character (Rouzina and Bloomfield, 1996, 1997). We and others found that the counterion pair correlation function $g(r)$ has its only peak at $r \approx a_z$, and is abutted by a correlation hole of comparable size. This pattern is more strongly expressed in systems with a higher average electrostatic repulsion between counterions relative to their thermal energy kT, as quantified by the 2-D coupling parameter:

$$\Gamma_2 = \frac{(ze)^2}{\epsilon a_z kT}. \tag{1}$$

Γ_2 = 0.7, 1.9, and 3.6 for 1-, 2-, and 3-valent counterions at the DNA surface, assuming the bulk value of the dielectric constant of water, ϵ = 78. Numerical studies show that even these moderate values of Γ_2 result in pronounced structure in $g(r)$.

In Fig. 1 we plot the effective phosphate charge felt by a z-valent cation at the distance r from a phosphate in the DNA backbone:

$$z_p(r) = 1 - g(r). \tag{2}$$

To obtain this figure we used numerical results for $g(r)$ with corresponding Γ_2 values (Figure 9 of Rouzina and Bloomfield, 1996), scaled with the appropriate a_z. We thus see that when B-DNA is screened by monovalent cations, each cation experiences complete neutralization of the phosphate charges beyond ~9 Å. At the same time, di- and trivalent cations at the DNA surface will phosphate neutralization only beyond ~13 Å and ~16 Å, respectively. It is for this reason that modeling the DNA double helix with neutral, or almost neutral, phosphates works well for monovalent counterion atmosphere (Zhurkin et al, 1978, 1980; Lavery et al, 1986 a,b), but should fail for higher valent counterions.

In our further considerations it will be important that, in the cases in which the electrostatic energy of cation interaction with the surrounding phosphates,

$$E_{el}(r) = -\frac{e^2 z z_p(r)}{\epsilon r}, \tag{3}$$

is significant (i.e., large with respect to kT), the effective phosphate charge z_p felt by the cation is close to its full charge of −1.

Distance-Dependent Dielectric Function

Equation 3 underestimates the electrostatic interaction between counterions by using the bulk value of the dielectric constant $\epsilon_{r\to\infty} = D = 78$, which is appropriate only for large ion separations. At short separations, the effective dielectric constant should become much smaller, and tend to its vacuum value of 1 in the limit of ion contact. This motivates use of the semiempirical distance-dependent dielectric function $\epsilon(r)$ (Hingerty et al., 1985):

$$\epsilon(r) = D - \frac{D-1}{2}\left[\left(\frac{rC}{H}\right)^2 + 2\frac{rC}{H} + 2\right]e^{-rC/H} \tag{4}$$

Here $C = 2.674$ is a constant, and $H = 7.5$ Å is the half-saturation length related to the size of the water molecule. Equation 4 combines experimental data on the strength of electrostatic interaction of close ion pairs in water with Debye-type analytical considerations. This sigmoidal dielectric function leads to a much shorter range of electrostatic interaction in water than in vacuum. Numerous modeling studies of DNA with either explicitly or implicitly included counterions have shown that this function adequately represents the short-range shielding effect of water near the DNA surface. Although a better grounded theory of Coulombic interactions in water at short distances is needed, the effect that we are considering in this study does not rely heavily on the particular shape of $\epsilon(r)$. The essential feature is the strong electrostatic interaction between ions at separations of 5–10 Å, which rapidly becomes weaker at longer distances.

Fig. 2 compares the electrostatic energy with those of the other major interactions, Lennard-Jones and hydrogen bonding. Nonbonded electrostatics is usually employed only at atomic separations beyond that at which hydrogen bond formation is possible, ~5 Å (Lavery et al., 1986b). It is evident that, at this separation, nonspecific electrostatics is still very strong relative to other interactions, and it has the longest range. The cation therefore can interact simultaneously via nonbonded electrostatics with multiple charges on the DNA. No exact atom positioning is required.

Electrostatics of Groove Closure

If DNA were a uniformly charged cylinder, its 2-D correlated counterion atmosphere described above would not prefer any particular position at the DNA surface. The actual arrangement of the DNA phosphate charges in two helical lines results in a slight preference for positioning of counterions near either a groove or a strand, depending on the size and charge distribution of the cation and the shape of the distance-dependent $\epsilon(r)$. If the possibility of DNA deformation by a cation is taken into account, the optimal electrostatic position of the cation will undoubtedly be in one of the collapsed grooves, i.e., in the region of highest unscreened phosphate concentration. To decide on the feasibility of such DNA deformation, we need to consider its energetics. The electrostatic energy benefit from such groove closure will depend on the cation structure. At the level of detail pertinent to the present discussion, we model the cationic ligand either as a hard sphere of radius δ and charge z at its center, or as a chain ligand with the z charges separated by d Å, which with $d = 5$ Å should be a suitable model for polyamines such as spermidine^{3+} or spermine^{4+}. We assume that the ligand is positioned at the groove entrance equidistant from the phosphate strands, which corresponds to the maximum electrostatic effect of the groove closure. The total charge on the surrounding phosphate groups is assumed to be equal to the cation charge. The difference in electrostatic energy of the cation-DNA interaction due to the groove closure will then be

$$E_{el}(W) = -e^2 f(z)\left[\frac{1}{\epsilon\left(\frac{W}{2}\right)\frac{W}{2}} - \frac{1}{\epsilon\left(\frac{W_0}{2}\right)\frac{W_0}{2}}\right]. \qquad (5)$$

W_0 and W are the unperturbed and diminished width of the groove, respectively. The factor $f(z)$ depends on the charge distribution of the cation. For a small compact cation, $f(z) \approx z^2$, whereas for a chain cation, $f(z) \approx z$. The electrostatic binding energy as a function of the major groove width, $E_{el}(W)$, is plotted in Fig. 3 for compact and chain ligands, with $z = 1$, 2, 3, and 4. For imperfectly correlated counterion atmosphere interactions across the unperturbed major groove, through the distance $W_0/2 = 10$ Å, there is attraction to the partially screened phosphates, whose charge scales with $z_p(r)$ (Eq. 2). But upon groove closure, the effective phosphate charge within the correla-

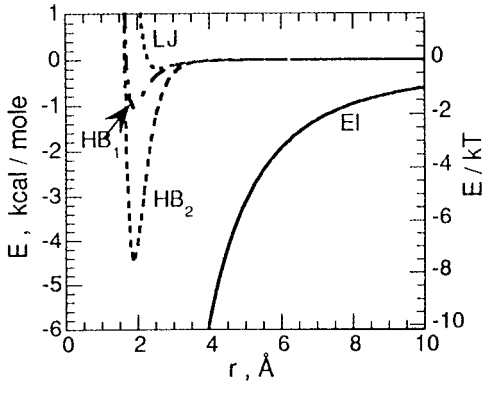

FIGURE 2 Typical pairwise interaction energies that may contribute to cation-DNA interaction. LJ, Lennard-Jones (Lavery et al., 1986b); HB_1, hydrogen bonding (Lavery et al., 1986b); HB_2, hydrogen bonding (Zhurkin et al., 1980); El, nonbonded electrostatic attraction between two monovalent charges (Eq. 3), with $\epsilon(r)$ given by Eq. 4.

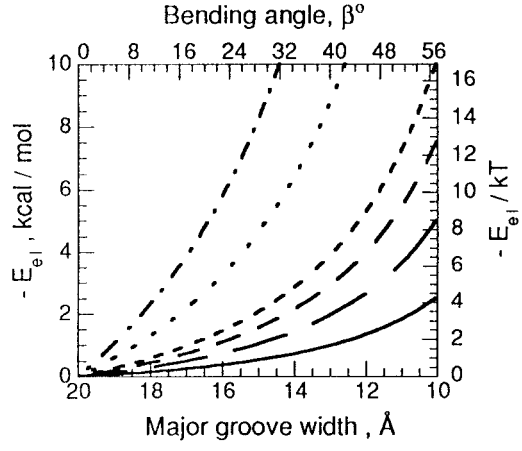

FIGURE 3 Electrostatic bending energy $E_{el}(W)$ for B-DNA with a z-valent cation at the center of the major groove entrance, as a function of the compressed groove width W according to Eq. 5. The top scale gives the bending angle as a function of W according to Eq. 8. The curves correspond to the following values of $f(z)$ in Eq. 5: solid line, 1; long dashes, 2; medium dashes, 3; short dashes, 4; dots, 9; dot-dash, 16.

tion hole should become equal to the cation charge. The electrostatic energy benefit of the cation-induced groove closure will then be somewhat larger than that given by Eq. 5.

BENDING ENERGETICS: ELECTROSTATIC AND ELASTIC CONTRIBUTIONS

Electrostatics is the only relatively long-range interaction between DNA and the cationic ligand that acts not just between particular pairs of atoms, but also affects a sequence containing several base pairs. Indeed, by pulling on neighboring phosphate strands across the major groove, electrostatics affects the conformation of at least 6 bp within the groove. The simplest macroscopic model of DNA bending, which considers independent roll and tilt of successive base pair dimers (Schellman, 1974) yields the elastic bending energy of a fragment containing N base pairs through an angle β:

$$E_{bN} = \frac{1}{2} g_N \beta_N^2. \tag{6}$$

The magnitude of the bending rigidity g_N should lie between its hinge value,

$$g_{hN} = \frac{P_0}{2bN} kT, \tag{7}$$

and the twofold larger isotropic limit $g_{iN} = 2g_{hN}$. Here $P_0 = 500$ Å is the high salt macroscopic persistence length of the B-DNA in monovalent buffer, $b = 3.4$ Å is the rise per base pair in B-DNA, and β_N is the bending angle in radians. It has been shown (Zhurkin, 1984) that bending in the groove direction is about an order of magnitude easier than it is in the direction of the sugar-phosphate strands. Therefore, a considerable part of the bending tends to concentrate within the base pair dimers bending into the groove, and the rest is distributed over all other steps (Sanghani et al., 1996).

Because bending of the DNA fragment between the phosphate strands into the groove takes advantage of the preferred bending direction and the possibility of distributing the bend over several base pairs, it is the most natural way for the DNA to deform. The bending rigidity should therefore be closer to the hinge model. Thus we can estimate that for $N = 1$ (one dimer), $g_{h1} = 73kT = 43$ kcal/mol; whereas for the $N = 6$ bp fragment within the major groove, $g_{h6} = 12kT = 7$ kcal/mol. This estimate agrees very well with the result of modeling the 14-mer (Boutonnet et al., 1993), which yields $g_6 = 7.8$ kcal/mol.

This means that the average bending angle due to the thermal fluctuations per 6 bp is about $\Delta\beta_6 = \sqrt{1/12} = 0.29 = 16°$. Furthermore, a bend of $36° = 6 \times 6°$ composed of six 6° bends of individual steps can be achieved without any significant perturbation of the B-DNA geometry, because all dihedral angles are within 15° of their average standard values (Zhurkin, 1984).

The bending angle in optimally bent DNA can be monotonically related to the groove width. A simple relationship, following from the mechanical model of a thick short rod compressed on one face at constant volume as shown in Fig. 4 *a*, is

$$W(\beta) = W_0 - R\beta, \tag{8}$$

where R is the radius of the DNA cylinder. In Fig. 4 *b* this simple prediction, with $W_0 = 20$ Å (without subtracting the size of the phosphate group) and $R = 10$ Å, is compared with the modeling result (Boutonnet et al., 1993). Agreement is excellent over the range of positive bending angles of interest to us.

If the cation is fixed in a position optimal for electrostatic bending, at the entrance to the major groove, then the angle-dependent components of the energy E of the bend are the electrostatic and the elastic:

$$E(\beta) = E_{el}(\beta) + \frac{1}{2} g_6 \beta^2, \tag{9}$$

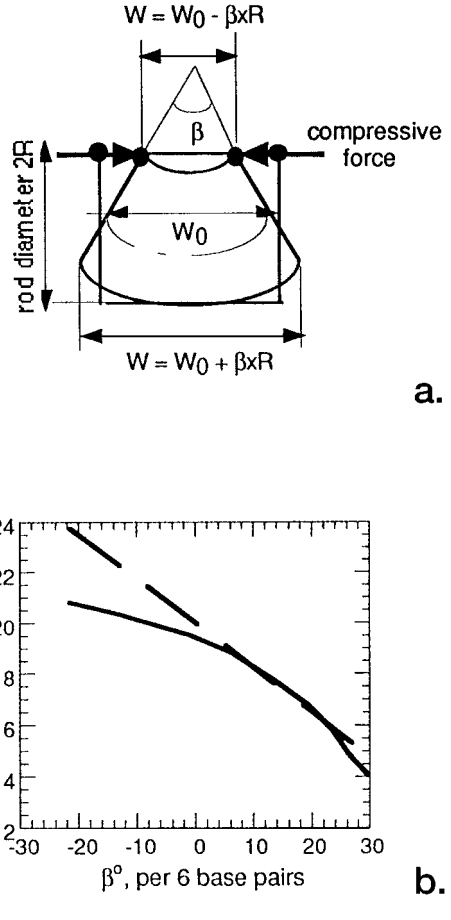

FIGURE 4 (*a*) Simple mechanical model for bending a short DNA fragment. Compressive force, represented by the bold arrows, is applied to the fragment sides on one face, producing a bend β. (*b*) Major groove width as a function of bending angle: dashed line, simple model (Eq. 8); solid line, numerical results (Boutonnet et al., 1993).

where $E_{el}(\beta)$ is given by Eq. 5, with the $W(\beta)$ dependence given by Eq. 8. The bending energy is given by Eq. 6, with $g = 12$ per 6 bp. The maximum stabilization energy E^* and the optimal angle β^* are found from the conditions

$$\frac{\partial E}{\partial \beta} = 0, \quad \beta^* = -\frac{1}{g}\frac{\partial E_{el}(\beta^*)}{\partial \beta}, \quad E^*_{el} = E_{el}(\beta^*). \qquad (10)$$

The particular value of the optimal bending angle depends on the distance dependence of the dielectric function. The absolute values of the bending and electrostatic energies as functions of bending angle are plotted in Fig. 5 for a monovalent counterion with three different models for $\epsilon(r)$; we used $W_0 = 20$ Å and $R = 10$ Å. We see that if the bulk value $\epsilon = 78$ is used everywhere, the electrostatic benefit from bending is negligible, and none of the effects discussed in this study could occur. On the other hand, the common approximation $\epsilon(r) = r$ (Å) clearly exaggerates the electrostatic effect, predicting that even a monovalent cation could collapse the major groove. The somewhat better grounded sigmoidal function (Eq. 4) results in an electrostatic energy that is too small to bend the DNA with a monovalent cation, but should be enough with a higher cationic charge.

Fig. 6 represents the total energy E according to Eq. 9, calculated for the sigmoidal dielectric function (Eq. 4), multiplied by the factors $f(z) = 1, 2, 3, 4, 9$, and 16 as in Eq. 5. We see that for $f(z) = 1$ and 2, a weak minimum in the total energy is observed at small bending angles. For more highly charged or more compact cations, the energy monotonically decreases with bending angle. This means that the DNA rigidity cannot balance the tendency of the cation to bend the helix, so that the DNA bends until its narrowed groove can no longer sterically accommodate the cation.

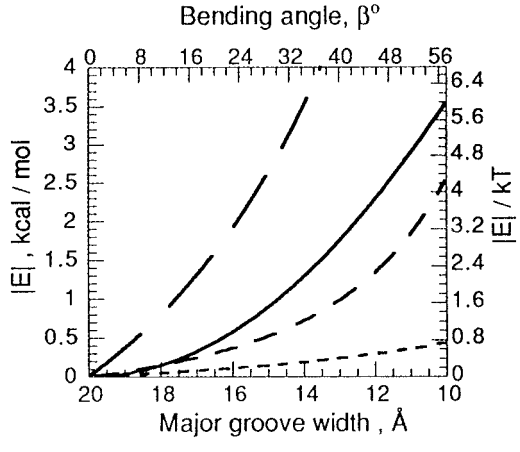

FIGURE 5 Bending and electrostatic energies as functions of major groove width and bending angle. Solid line, Absolute value of elastic bending energy $E_b(W)$ according to Eq. 6 for a 6-bp fragment with $g = 12$. Dashed lines, Absolute value of the electrostatic bending energy $E_{el}(W)$ for a monovalent cation according to Eq. 5, with three models of the dielectric function: short dashes, $\epsilon = 78$; medium dashes, $\epsilon(r)$ (Eq. 4); long dashes, $\epsilon = r$ (in Å).

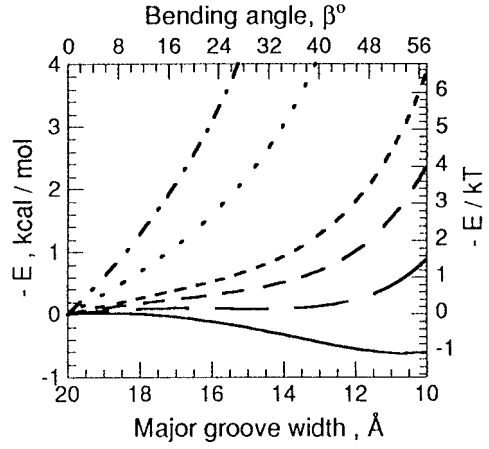

FIGURE 6 Dependence of total energy (Eq. 9), on groove width and bending angle. The bending energy is given by Eq. 6, with $g = 12$. The electrostatic energy is given by Eq. 5, with the curves corresponding to the following values of $f(z)$: solid line, 1; long dashes, 2; medium dashes, 3; short dashes, 4; dots, 9; dot-dash, 16.

The maximum sterically allowed bending angle β_{max} is related to the minimum groove width $W_{min} = W(\beta_{max})$ by Eq. 8. The minimum width is the sum of the phosphate diameter, 5.8 Å, and the (hydrated) ion diameter, 2δ, so

$$\beta_{max} = \frac{W_0 - W_{min}}{R} = \frac{20 - (5.8 + 2\delta)}{10}. \qquad (11)$$

In Table 1 we use estimates (Gessner et al., 1985; Paulsen et al., 1988) of the hydrated diameters of some cations of interest to calculate W_{min} and β_{max}. We also estimate the electrostatic energy, $E_{el}(\beta_{max})$, corresponding to the maximum bend and the energetic cost of the related elastic deformation, $E_b(\beta_{max})$. The sum of these two energies yields the electrostatic stabilization of the bend, $E(\beta_{max})$, which ranges between $-2kT$ and $-10kT$ per cation.

This conclusion is outrageous: we predict that every bound, compact, divalent cation should be able to bend B-DNA by 20° to 40°! If this were true, the persistence length of DNA with any multivalent cation should be 5–10 Å, rather then 150–300 Å. What is wrong with this physical picture?

TABLE 1 Parameters for maximum sterically allowed DNA bending

Cation	2δ (Å)	W_{min} (Å)	β^*_{max} (°)	E^*_{el}/kT	E^*_b/kT	E^*/kT
Na^+	5.6*	11.4	49	−2.4	4.4	2
Mg^{2+}	10.6*	16.4	21	−2.7	0.9	−1.8
Ca^{2+}	9.4*	15.2	27	−3.5	1.4	−2.1
$CoHex^{3+}$	6#	11.8	46	−14	3.9	−10.1
$Putrescine^{2+}$, $spermidine^{3+}$, $spermine^{4+}$	6–8*	12–13	40–45	−(4–7)	2.9–3.7	−(1.1–3.3)

*Paulsen et al. (1988).
#Gessner et al. (1985).

DYNAMIC ASPECTS OF DNA BENDING

The main conclusion of the previous section is that a cation positioned centrally at the major groove entrance should most effectively induce B-DNA bending. Other cation positions, deep within the groove or on a strand, result in much weaker electrostatic energy of groove closure, which can cause minor DNA deformation but will not result in significant bending. This conclusion is based on a static picture, however, whereas the problem is, in fact, a dynamic one.

For the type of cations considered here, it is known from NMR experiments (Braunlin et al., 1991, 1992; Wemmer et al., 1985; Xu et al., 1993a) that the majority remain highly mobile when bound to DNA. At the same time, molecular modeling studies (Lavery et al., 1986a; Zakrzewska and Pullman, 1986; Zhurkin et al., 1980) that place a single cation in various locations on DNA show multiple van der Waals and hydrogen bonding contacts. The energies of these contacts are similar along a groove or strand, and are moderate compared to the free energy of polyelectrolyte binding to the uniformly charged cylinder. Therefore, "specific" interactions, which also include a component of electrostatic energy due to the discrete helical phosphate charge arrangement (Lamm et al., 1994), lower the cation energy but do not substantially inhibit its motion along the surface. Instead, a spectrum of bound energy states is created, each characterized by some modestly reduced mobility.

When many multivalent cations are bound to a DNA molecule, the lower energy states become saturated both sterically and through mutual electrostatic repulsion between the cations. In addition, a small fraction of the DNA charge is always neutralized by weakly bound cations beyond the Debye screening length. Between the strongly and weakly bound cations are a few, bound strongly but nonspecifically, just at the polyelectrolyte level. A cation centered at the major groove entrance is at this energy level, because it lacks all van der Waals and hydrogen bond contacts until the groove is collapsed. The polyelectrolyte level is essentially unoccupied until all lower energy states are filled. A cation can move to this level by an activated process, but its lifetime there will be too short for the relatively slow process of DNA bending to occur. The ability to bend DNA is thus limited to the small number of cations that do not need activation energy to get to the major groove entrance. Such cations appear at high ratios of bound cation to DNA phosphate.

These cations are highly mobile, whereas DNA bending is several orders of magnitude slower. The characteristic residence time of an electrostatically nonspecifically bound cation near any nucleotide residue is 10–30 ps (Xu et al., 1993a), only a few times longer than for the same ion in bulk solution. The typical time for DNA bending is 0.1–1 μs for lengths of 30–100 bp (Porschke, 1986), increasing approximately as the third power of the DNA length. The question then arises: Will the DNA be able to bend around such a rapidly moving cation? In this section we show that it can, but that cation localization within the bend will have an entropic cost that will considerably lower the stability of the bent state.

The large difference in time scales allows us to describe the counterion position as a time-averaged distribution function $h(x)$ of its coordinate x on the DNA surface measured along the DNA axis. The $h(x)$ function can be found for every DNA conformation, characterized by the bending angle β into the major groove. The DNA conformation also varies, but on a much longer time scale, so that $h(x)$ for the mobile cation is in equilibrium at any DNA conformation. This approach is an example of the adiabatic approximation (Landau and Lifshitz, 1976).

The cation density function $h(x)$ should have a maximum at the center of the bent fragment between the two phosphate strands, where $x = 0$, and can be characterized with the single parameter Δx, the width of the distribution:

$$\Delta x = \langle \Delta x^2 \rangle^{1/2} = \left[\int x^2 h(x) dx \right]^{1/2}. \tag{12}$$

The degree of cation localization is then represented by the ratio

$$\Delta = \Delta x / W_0, \tag{13}$$

where W_0 is the unperturbed groove width.

The electrostatic energy of DNA bending $E_{el}(\beta, \Delta)$ is now a function not only of the bending angle β, but also of Δ. It has a minimum $E_{el}(\beta, 0)$ (calculated in the previous section as $E_{el}(\beta)$) for a stationary cation fixed midway between the strands, and it should vanish for $\Delta = 1$, when the cation is uniformly smeared over the major groove. A simple but adequate function that has these properties is

$$E_{el}(\beta, \Delta) = E_{el}(\beta, 0)[1 - \Delta^2]. \tag{14}$$

A more refined treatment, taking into account the steepness of the $\epsilon(r)$ function and the shape of $h(x)$, would multiply Δ^2 by a coefficient of order unity, and would have only a minor effect on our conclusions.

The electrostatic interaction tends to localize the cation at the groove center, but localization has an entropic cost ΔS. If a mobile ligand of length l_0 is localized within the length Δx,

$$-T\Delta S = -kT \ln\left(\frac{\Delta x}{l_0}\right) = -kT \ln(6 q_{i0} \Delta), \tag{15}$$

where q_{i0} is the frequency of localizable cation per base pair. The total free energy stabilizing the bent DNA conformation, in kT units, is then

$$G(\beta, \Delta) = E_{el}(\beta, 0)[1 - \Delta^2] + \frac{1}{2} g_6 \beta^2 - \frac{1}{2} \ln \Delta^2 - \ln(6 q_{i0}). \tag{16}$$

Minimizing the free energy with respect to Δ^2 at fixed angle β, one obtains

$$\Delta^2(\beta) = -\frac{1}{2E_{el}(\beta)}. \tag{17}$$

In accord with intuition, stronger electrostatic energy results in smaller Δ, i.e., it produces stronger localization; this is opposed by thermal energy.

Substituting Eq. 17 into Eq. 16, we obtain the optimal free energy of the bend,

$$G(\beta) = E_{el} + \frac{1}{2}g_6\beta^2 + \frac{1}{2}[\ln(-2E_{el}) + 1] - \ln(6q_{i0}), \quad (18)$$

which is similar to the energy (Eq. 9), except for the unfavorable entropic contribution from the last two terms. The first is the entropy of localizing the cation within the groove, and the second is due to the low concentration of cations that can be self-localized.

For a rapidly saturating sigmoidal dielectric function, there will be, just as in the static case, no extremum of G with respect to β. The free energy will decrease until the bend angle reaches its largest sterically allowed value β^*. G^* as a function of E_{el^*} (Eq. 18) is plotted in Fig. 7. We see that the high entropic cost of cation localization creates a critical condition for the cation stability, i.e., $G^* < 0$ is satisfied only for $E_{el^*} < E_{cr}$. Cations with weaker electrostatic interaction cause no bending at all, whereas cations that interact more strongly bend DNA by the large angle β^*. This is in contrast to the static case in which any multivalent cation can induce some bending. The behavior described here is a typical example of a polaron, in which the particle creates a deformation within the medium through which it moves, and in turn is self-localized within this deformation, thus maximizing the interaction and stabilizing the deformation.

The critical energy E_{cr} depends on q_{i0}, the frequency of cations that can be self-localized. This, in turn, depends not only on the cation type, but also on the DNA sequence. The less specific is cation binding to sequences near the one to be bent, the more cations are available for the electrostatic self-localization. When the bend is completed, the cation can adjust its conformation to form all possible hydrogen bonds to the phosphate oxygens within the major groove. The strength of such an interaction will be comparable to or smaller than the hydrogen bonding of the cation to specific sites on unbent DNA. Hydrogen bonding to the phosphates can substantially increase the stability of a bend, but because of the short range of the hydrogen bond, it cannot drive the groove collapse.

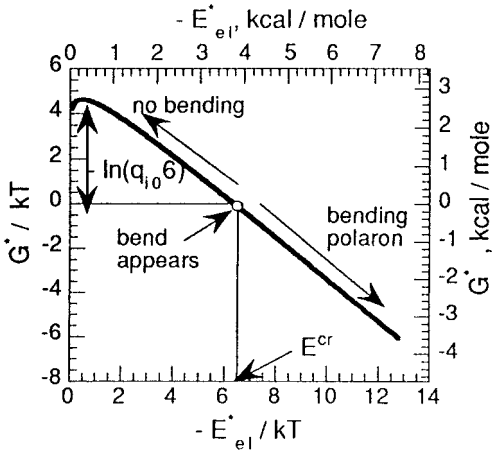

FIGURE 7 Free energy G^* of a cation-induced bending polaron as a function of its maximum electrostatic energy E^*_{el}, as calculated from Eq. 18, with $q_{i0} = 0.002$.

Because the cations bound to DNA have a continuous spectrum of energies and mobilities, there is a question of how effective the electrostatic coupling between these cations and the induced DNA deformation will be. It appears that coupling is optimal in two limiting cases, when cation diffusion is either much slower or much faster than the bending motions of the DNA. In the first case the DNA always has time to reach its optimal bent conformation. In the second case the cation instantaneously adjusts to the DNA conformation, driving it to the optimal bent configuration, but at an additional cost of the entropy of cationic localization. In the intermediate situation, when the time scales of DNA and cation motion are comparable, electrostatic coupling between them is weak, and even a highly charged cation is unable to bend DNA. Thus cations positioned somewhere other than at the major groove entrance are not only electrostatically less potent in inducing DNA bends, but are also less effective, because of weak dynamic coupling.

EFFECT OF MULTIVALENT CATIONS ON DNA PERSISTENCE LENGTH

As noted in the Introduction, multivalent cations can dramatically reduce the persistence length of B-DNA. Our interpretation of this phenomenon is that the multivalent cations introduce infrequent but strong bends in the DNA. The maximum frequency of such bends per base pair, q_{i0}, is small and depends on the DNA sequence, whereas the bend angle is $20-40°$ and depends mainly on the size of the cation. The bend is smoothly distributed over $\sim$6 bp and is directed toward the major groove at the center of the bent fragment. Positions of the self-localized cations, and therefore the bend directions, are uncorreleted.

The persistence length P of a polymer that bends according to a hinge mechanism (Schellman, 1974) is related to the length per base b and the mean-square bending angle per base pair β as

$$P = \frac{2b}{\langle\beta^2\rangle}. \quad (19)$$

In high ionic strength sodium buffer, the persistence length

$$P_0 = \frac{2b}{\langle\beta_0^2\rangle} \quad (20)$$

is the result of sequence-dependent static and dynamic contributions (Trifonov et al., 1987). From the known value of $P_0 = 500$ Å, one estimates $\langle\beta_0^2\rangle^{1/2} = 0.12$ rad $= 6.7°$.

The reduction of P by multivalent cations means additional DNA bending induced by these cations. If a cation induces a bend of angle β_i in a random direction every q_i base pairs, and this bending is statistically independent of bending in the absence of multivalent cations, then

$$\langle\beta^2\rangle = \langle\beta_0^2\rangle + q_i\langle\beta_i^2\rangle. \quad (21)$$

The additional bending is characterized by the persistence length P_i,

$$P_i = \frac{2b}{q_i\langle\beta_i^2\rangle}. \quad (22)$$

We can then rewrite Eqs. 19 and 21 in the form

$$\frac{1}{P} = \frac{1}{P_0} + \frac{1}{P_i}, \quad (23)$$

so that the change in P in the mixed salt relative to the monovalent buffer value P_0 is

$$\frac{P}{P_0} = \frac{1}{1 + P_0/P_i} = \frac{1}{1 + q_i\langle\beta_i^2\rangle/\langle\beta_0^2\rangle}. \quad (24)$$

Experimentally, the persistence length decreases as multivalent cations replace monovalent cations at the DNA surface. We attempt to account for that by assuming, to a first approximation, that the probability of a bend per base pair is proportional to the number of cations bound per base pair, Θ_z:

$$q_i = q_{i0}\Theta_z. \quad (25)$$

The fractional occupancy Θ_z varies from 0 to $2/z$ and is determined by the bulk concentrations $[L^{z+}]$ and $[Na^+]$ through the relationship (Rouzina and Bloomfield, 1997)

$$\frac{z\Theta_L}{2} = \frac{[L^{z+}]}{[Na^+]^z} n_s^{z-1}\left(1 - \frac{z\Theta_L}{2}\right)^z, \quad (26)$$

where n_s is the concentration of the cation at the DNA surface, 1 M or greater. The experimental data can be fitted to Eq. 24 with respect to the single parameter $q_{i0}\langle\beta_i^2\rangle$ while taking into account Eqs. 25 and 26. The fits are shown in Fig. 8, and the fitting parameters are given in Table 2. If we assume that every bound cation produces an equivalent bend, so that $q_{i0} = 2/z$, then the minimum angle needed to account for the observed reduction in P is given in the fourth column of the table. These angles are comparable to the high monovalent salt rms angle of 6°–7°; but a relatively small bend at each base pair induced by multivalent cations is unlikely for the reasons given in the previous section. The alternative picture that bending is stronger but less frequent gives the probabilities q_{i0} in the last column of Table 2 if we assume a reasonable value $\beta_i = 30°$. The probability is highest for $CoHex^{3+}$ and is comparable to the frequency of a GG step to be expected in random sequence DNA.

The frequency of bending is substantially lower for the other three cations. Moreover, the fitted curves for these ions are shifted toward higher values of $[L^{z+}]/[Na^+]^z$, particularly for the polyamines. This shift cannot be attributed to a difference in binding constants, i.e., to a difference in n_s in Eq. 26, because it is known from direct measurement (Plum and Bloomfield, 1988) that $CoHex^{3+}$ and $spermidine^{3+}$ have similar constants for binding to B-DNA, whereas to explain the relative shift of the curves in Fig. 8 they would have to be 30-fold different. A more plausible explanation is that $CoHex^{3+}$ provokes DNA bending at low concentrations because of preferential binding to GG sequences in the major groove. The GG-bound cations do not bend the DNA themselves, but rather create the sites at which the DNA can be bent upon subsequent $CoHex^{3+}$ accumulation. Therefore, the experimental change in persistence length parallels the $CoHex^{3+}$ titration curve, and the maximum bend frequency corresponds to that of the GG steps. On the other hand, polyamines or Mg^{2+} have no strong affinity for any sequence, and bend DNA only at the later stages of titration, when all low-energy binding levels are filled and the residual highly mobile cations can self-localize anywhere in the major groove.

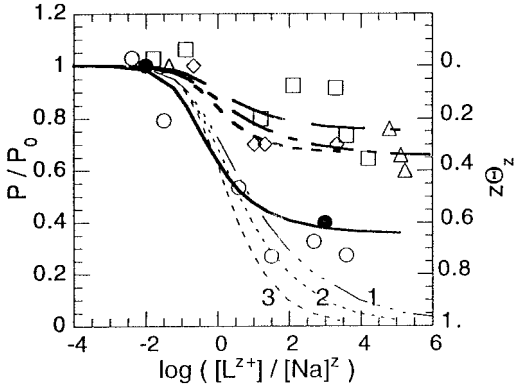

FIGURE 8 Persistence length P of B-DNA, relative to its high salt value P_0, in the presence of multivalent cations. The solution composition is represented by the reduced ligand concentration as in Eq. 26. The experimental points are for solutions with the following multivalent cations: ○, $CoHex^{3+}$ (Baumann et al., 1997; Baumann and Bloomfield, unpublished); ●, $CoHex^{3+}$ (Porschke, 1986); ◊, Mg^{2+} (Porschke, 1986); ❐, $spermidine^{3+}$ (Baumann et al., 1997); △, $spermine^{4+}$ (Porschke, 1986). The heavy lines, corresponding to the left ordinate, are fits to Eq. 24 with respect to the parameter $q_{i0}\langle\beta_i^2\rangle$, taking into account Eqs. 25 and 26. The fitted values of $q_{i0}\langle\beta_i^2\rangle$ are given in Table 2. The light lines, corresponding to the right ordinate, show the fractional DNA charge neutralization by z-valent cation. For both sets of lines, the cation valence z = 1, 2, and 3 from top to bottom.

TABLE 2 Bending parameters with multivalent cations from data on DNA persistence length

Ion	$(P/P_0)_{min}$	$q_{i0}\langle\beta_i^2\rangle$	$\beta_{i,min}$*	q_{i0}#
Mg^{2+}	0.70	0.006	5.5°	0.022
$CoHex^{3+}$	0.35	0.267	11.5°	0.098
$Spermidine^{3+}$	0.75	0.005	4.0°	0.018
$Spermine^{4+}$	0.65	0.008	7.1°	0.028

*Assumes $q_{i0} = 2/z$.
#Assumes $\beta_i = 30°$.

The maximum bend frequency q_{i0} in Table 2 for all cation species except $CoHex^{3+}$ is ~0.02. If this is the fraction of cations that can be electrostatically self-localized, then the entropy of such localization is $-\ln(0.02 \times 6) \approx 2kT$ per cation. This magnitude is similar to the stabilization energy of the static bend by these cations, estimated in the last column of Table 1, supporting the idea that such infrequent bending by these multivalent cations is possible. More detailed quantitative estimates are unjustified, in the absence of a better-grounded characterization of the strength of electrostatic interaction through a thin water layer.

COMPARISON WITH EXPERIMENT

Solution Experiments

According to our theory, DNA electrostatic bending is strong but smooth. Bends are distributed over ~6 bp and do not significantly perturb the B-DNA helical structure. Such bending should not measurably affect DNA electronic or vibrational spectra, but should be evident in techniques for measuring DNA curvature such as electrooptics, gel electrophoresis, cyclization, and single molecule stretching experiments. It might also show up as a reduction in cation mobility in NMR experiments. These expectations are borne out by results in the literature.

Evidence of strong, stable DNA bending in the presence of multivalent cations without any significant B-DNA helix perturbation was provided by the electrooptical study of Pörschke (1986). Gel electrophoretic measurements (Brukner et al., 1994) for the first time characterized DNA bending toward the major groove in GGGCCC-containing sequences, induced by metal cations in the order $Ca^{2+} > Mg^{2+} > Zn^{2+}$. The absolute value of the effect was not measured, because cations also increased the bending of the control AA/TT-containing DNA fragment. The curvature induced in the AT-rich sequences, however, was much smaller, in accord with our expectations. Indirect evidence of reduced DNA rigidity in the presence of Mg^{2+} and $spermidine^{3+}$ comes from the increased probability of DNA cyclization in the presence of these cations (Rybenkov et al., 1997). Single DNA molecule stretching experiments (Baumann et al., 1997; Wang et al., 1997) also give clear evidence of reduction of persistence length, most likely caused by bending, by multivalent cations.

Combined NMR and CD studies of $CoHex^{3+}$-DNA interaction by Braunlin and co-workers (Braunlin and Xu, 1992; Xu et al., 1993a) cannot provide direct evidence of bending, but are compatible with our physical picture. Three classes of $CoHex^{3+}$ sites of binding to both genomic DNA and various short oligomers were distinguished by NMR; the oligomers were studied by circular dichroism (CD) as well. The first class of sites bound $CoHex^{3+}$ strongly, inhibiting its independent rotational motion. The DNA that exhibited this behavior had very high guanine content: the oligomers had stretches of two or more same-strand guanines, and the genomic DNA was *M. lysodeikticus*, with 72% GC. The CD changes caused by $CoHex^{3+}$ in these oligomers suggested a transition from B- to A-conformation (Xu et al., 1993b), which would involve the same major groove collapse that we postulate is involved in bending. $Spermidine^{3+}$ and Mg^{2+} cations did not produce the B-to-A transition in the sequence d(CCCCGGGG), but were significantly immobilized by it (Braunlin et al., 1991; Xu et al., 1993b). Both ions induced moderate changes in the CD spectrum toward the A form, less so for Mg^{2+}, indicating possible B-DNA bending by major groove collapse.

Binding to the second class of sites, seen in all of the genomic DNAs and in AT-rich oligomers, slowed $CoHex^{3+}$ rotational motion only about fivefold relative to its solution state, and did not cause any CD change. This is, we think, because the $CoHex^{3+}$ molecule spends most of its time in the vicinity of the narrow minor groove of the AT-rich sequence, where it remains mobile. $CoHex^{3+}$ molecules in this state are unable to collapse the major groove. The third class of sites is seen in all genomic DNAs and in oligomers with no same-strand runs of guanines and no AT-rich sequences. It localizes the cation but does not significantly inhibit its rotation or involve major changes in CD spectrum. This behavior is compatible with $CoHex^{3+}$ self-localization and DNA bending into the major groove at the center of the sequence.

Crystallography

In the few cases in which multivalent cations have been unambiguously determined within crystals of DNA oligomers (Bancroft et al., 1994; Drew and Dickerson, 1981; Gao et al., 1995; Nunn and Neidle, 1996; Quigley et al., 1978; Robinson and Wang, 1996; Williams et al., 1990), they were either bound to the electrophilic sites on the bases or located in regions of high concentration of phosphates, due, in particular, to a narrowed B-DNA major groove. The molecules with strongly A-philic DNA sequences due to same-strand runs of guanines all underwent the B-to-A transition. The local geometries of the major grooves in A-DNA and in B-DNA bent toward the major groove are very similar, and can be stabilized by the same cationic interactions.

In all cases in which a strongly narrowed or collapsed major groove was observed, a multivalent cation electrostatically bridged the phosphate strands. A second cation bound to a same-strand run of GG bases was observed with $CoHex^{3+}$ as the counterion in A-DNA (Gao et al., 1995) and in tRNA (Hingerty et al., 1982). Similar results were obtained by NMR (Robinson and Wang, 1996) and in a recent molecular dynamics simulation (Cheatham and Kollman, 1997). When the sequence did not have same-strand guanine runs, but had high A-philicity as a DNA/RNA hybrid, only the phosphate-bound $CoHex^{3+}$ was observed. Therefore we conclude that it is the phosphate-bound cation that is critical for stabilization of the narrow major groove. $Spermine^{4+}$ could not be located in the crystal structure of

A-form d(ACCGGCCGGT) (Gao et al., 1995), but it was bound exclusively to the phosphates in the crystal structure of the chimera r(C)d(CGGCGCCG)r(G) (Ban et al., 1994).

Molecular Modeling Studies

Although it is conceptually simple, DNA electrostatic bending is not easy to model at the atomic level, because it requires an explicit accounting of electrostatic interactions between the flexible DNA, the multivalent cationic ligand, and mobile counterions. Early indications of the type of DNA bending proposed in this study were observed in molecular mechanics calculations of DNA with putrescine^{2+} (Lavery et al., 1986a) and spermine^{4+} (Zakrzewska and Pullman, 1986).

The putrescine study (Lavery et al., 1986a) considered the binding of the divalent polyamine to d($G_{15} \cdot C_{15}$) and d($A_{15} \cdot T_{15}$) in the presence of mobile Na^+ counterions. It was found that increasing the number of putrescine^{2+} per DNA resulted in switching the favored ligand position from deep in the minor groove of straight DNA to the entrance of the major groove in bent DNA. Simultaneous switching of all putrescine positions resulted from the helical symmetry imposed by the JUMNA model of DNA. In this simulation, the G · C molecule bent more easily than the A · T, because the putrescine in the minor groove of straight DNA formed a stronger bond to A · T.

A minor groove binding preference on straight B-DNA seems to be a general property of small linear polycations, according to molecular mechanics simulations with polyamines (Lavery et al., 1986a; Zakrzewska and Pullman, 1986; Zhurkin et al., 1980) and cationic antibiotics (Duong and Zakrzewska, 1997; Randrianarivelo et al., 1989; Zakrzewska et al., 1987). For both classes of molecules, a preference to bind to AT-rich sequences in the minor groove was observed. This preference is of electrostatic origin and is due to the narrower minor groove of AT-rich, relative to GC-rich, sequences.

The preference for minor groove binding to AT sequences determines the sequence specificity of electrostatic bending by multivalent cations predicted in the present study. The deeper potential well within the minor groove can accommodate more bound cations, assuming that they are sterically able to fit (linear polycations can, CoHex^{3+} cannot). Fewer of them are therefore available for self-localization at the major groove entrance. The binding strength is less for GC sequences than for AT, making GC-rich sequences more bendable. Such specificity will, of course, be manifested only in the absence of other, stronger specific binding effects.

Calculations with spermine^{4+} (Zakrzewska and Pullman, 1986) show that when nonbonded electrostatic is considered, the preferred spermine location is always in the region of highest phosphate concentration: in the minor groove of B-DNA, in the narrow major groove of A-DNA, in the region of major groove narrowing in the B-DNA Dickerson dodecamer, and in the high phosphate concentration regions of tRNA. The studies of Feuerstein et al. (1986, 1989, 1990) showed strong deformation of DNA by spermine^{4+} in the major groove, but we believe the effect is exaggerated because of their use of the $\epsilon(r) = r$ dielectric function. A B $\rightarrow$ A transition induced by CoHex^{3+} interaction with an A-philic DNA sequence was observed in a recent molecular dynamics simulation (Cheatham and Kollman, 1997).

SUMMARY AND DISCUSSION

We have shown that small, mobile, multivalent cations that bind nonspecifically to B-DNA can induce strong but infrequent bending. This bending is a result of the self-localization of individual cations at the major groove entrance, accompanied by collapse of the groove and DNA bending toward the cation. Such a "bending polaron" is driven by the nonbonded electrostatic attraction between the compact cationic charge and the bare phosphates from both strands of the collapsed groove. It is destabilized by the high entropic cost of confining the cation, which would otherwise be delocalized along the outer surface of the unbent DNA. The number of cations available for self-localization at the major groove is very limited, because most of them bind more strongly and with lower mobility to other regions on the DNA. They are then unable to bend the DNA, because their lifetime at the major groove entrance is much shorter than the typical DNA bending time. This leads to a significantly lower stability of the bends, as well as a low frequency. Another consequence of the very different time scales of the cation and DNA motions is that only those cations with electrostatic interaction stronger than some critical value will cause DNA bending. The cation should be at least divalent, and its charge should be compact.

The fraction of cations that cause DNA bending depends not only on cation type, but also on DNA sequence. AT-rich DNA is calculated to hold a greater number of linear multivalent cations, such as polyamines, near its narrow minor groove (Lavery et al., 1986a), so that fewer are available for localization within the major groove. We therefore predict that electrostatic bending will appear mostly at the last stages of DNA titration with such cations, and that bending will be greater in GC-rich than in AT-rich DNA.

Another example of dependence on DNA sequence is consecutive same-strand guanines. The only sterically accessible major groove sites susceptible to electrophilic attack by small cations are the N^7 and O^6 of guanine (Pullman et al., 1982). It appears that two successive guanines create a strong major groove site with four potential hydrogen bonds. Various multivalent cations use this binding site with different efficiency: CoHex^{3+} binds strongly, whereas spermidine^{3+} and spermine^{4+} do not (Gao et al., 1995). Binding of CoHex^{3+} deep within the major groove narrows this groove, and increases the probability of self-localization of a second cation between the strands, which completes the groove collapse. Therefore, the probability of bending of CoHex^{3+} correlates with the frequency of GG steps in the DNA sequence.

An important point is that multivalent cations stabilize the narrow major groove of A-DNA and of bent B-DNA through the same electrostatic interaction with the phosphates. For A-philic sequences this interaction drives the B → A transition, whereas for other sequences, B-DNA bending into the major groove is energetically favored.

A cationic ligand with high binding specificity will not cause significant DNA bending, unless its binding site is within the DNA major groove. A good example is the cationic antibiotic netropsin, which binds strongly along the B-DNA minor groove, rigidifying and straightening the DNA rather than bending it (Duong and Zakrzewska, 1997). On the other hand, the major groove-binding cationic α-helices seem to wrap the DNA around themselves (Fisher et al., 1992; Kerppola and Curran, 1991; Mondragon and Harrison, 1991). An interesting implication of our theory of bending is that the less specific the cation binding to DNA, the more bending it can cause, as long as it can fit into the major groove. This prediction remains to be tested.

The electrostatic DNA bending angle is determined primarily by the cation size, which has to fit the collapsed major groove. This is because the bending rigidity of B-DNA is insufficient to balance the strong electrostatic energy causing the bend. Such a bend can easily reach 30° or more, smoothly distributed over the 6 bp within the major groove. Therefore the B-DNA deformation within the bend remains moderate, and may not manifest itself in spectral measurements.

The stability of electrostatically induced bends is expected to vary greatly depending on cation, DNA sequence, and ratio of cation to DNA phosphate concentrations. In some cases bending will be transient and observable only with time-averaged solution measurements or fast spectroscopic technics. In other cases cation-induced bending will be very stable and will be seen even in crystal structures. At the present time there exists a small body of experimental evidence supporting this picture of DNA bending by small, mobile, multivalent cations. More data are clearly needed for the unambiguous characterization of such bends.

This research was supported in part by National Institutes of Health research grant GM28093.

REFERENCES

Anderson, C. F., and M. T. Record, Jr. 1990. Ion distributions around DNA and other cylindrical polyions: theoretical descriptions and physical implications. *Annu. Rev. Biophys. Biophys. Chem.* 19:423–465.

Andreasson, B., L. Nordenskiöld, W. H. Braunlin, J. Schultz, and P. Stilbs. 1993. Localized interaction of the polyamine methylspermidine with double-helical DNA as monitored by ^{1}H NMR self-diffusion measurements. *Biochemistry.* 32:961–967.

Attard, P., D. J. Mitchell, and B. W. Ninham. 1988. Beyond Poisson-Boltzmann: images and correlations in the electric double layer. I. Counterions only. *J. Chem. Phys.* 88:4987–4996.

Baase, W. A., P. W. Staskus, and S. A. Allison. 1984. Precollapse of T7 DNA by spermidine at low ionic strength: a linear dichroism and intrinsic viscosity study. *Biopolymers.* 23:2835–2851.

Ban, C., B. Ramakrishnan, and M. Sundaralingam. 1994. Crystal structure of the highly distorted chimeric decamer r(C)d(CGGCGCCG)r(G) · spermine complex—spermine binding to phosphate only and minor groove tertiary base-pairing. *Nucleic Acids Res.* 22:5466–5476.

Bancroft, D., L. Williams, A. Rich, and M. Egli. 1994. The low-temperature crystal structure of the pure-spermine form of Z-DNA reveals binding of a spermine molecule in the minor groove. *Biochemistry.* 33:1073–1086.

Baumann, C., S. Smith, V. Bloomfield, and C. Bustamante. 1997. Ionic effects on the elasticity of single DNA molecules. *Proc. Natl. Acad. Sci. USA.* 94:6185–6190.

Berggren, E., L. Nordenskiöld, and W. H. Braunlin. 1992. Interpretation of ^{25}Mg spin relaxation in Mg-DNA solutions: temperature variation and chemical exchange effects. *Biopolymers.* 32:1339–1350.

Boutonnet, N., X. Hui, and K. Zakrzewska. 1993. Looking into the grooves of DNA. *Biopolymers.* 33:479–490.

Braunlin, W. H., T. Drakenberg, and L. Nordenskiöld. 1992. Ca^{2+} binding environments on natural and synthetic polymeric DNA's. *J. Biomol. Struct. Dyn.* 10:333–343.

Braunlin, W. H., L. Nordenskiöld, and T. Drakenberg. 1991. A reexamination of $^{25}Mg^{2+}$ NMR in DNA solution: site heterogeneity and cation competition effects. *Biopolymers.* 31:1343–1346.

Braunlin, W. H., and Q. Xu. 1992. Hexaamminecobalt(III) binding environments on double-helical DNA. *Biopolymers.* 32:1703–1711.

Brukner, I., S. Susic, M. Dlakic, A. Savic, and S. Pongor. 1994. Physiological concentration of magnesium ions induces a strong macroscopic curvature in GGGCCC-containing DNA. *J. Mol. Biol.* 236:26–32.

Cheatham, T., III, and P. Kollman. 1997. Insight into stabilization of A-DNA from molecular dynamics simulation performed in aqueous solvent in the presence of cobalt hexaamine or ethenol. *J. Biomol. Struct. Dyn.* 14:785–786 (Abstr.).

Drew, H. R., and R. E. Dickerson. 1981. Structure of a B-DNA dodecamer. III. Geometry of hydration. *J. Mol. Biol.* 151:535–556.

Duguid, J., V. A. Bloomfield, J. Benevides, and G. J. Thomas, Jr. 1993. Raman spectroscopy of DNA-metal complexes. I. Interactions and conformational effects of the divalent cations: Mg, Ca, Sr, Ba, Mn, Co, Ni, Cu, Pd, and Cd. *Biophys. J.* 65:1916–1928.

Duong, T. H., and K. Zakrzewska. 1997. Influence of drug binding on DNA flexibility—a normal mode analysis. *J. Biomol. Struct. Dyn.* 14: 691.

Elcock, A. H., and J. A. McCammon. 1996. The low dielectric interior of proteins is sufficient to cause major structural changes in DNA on association. *J. Am. Chem. Soc.* 118:3787–3788.

Feuerstein, B. G., N. Pattabiraman, and L. J. Marton. 1986. Spermine-DNA interactions: a theoretical study. *Proc. Natl. Acad. Sci. USA.* 83:5948–5952.

Feuerstein, B. G., N. Pattabiraman, and L. J. Marton. 1989. Molecular dynamics of spermine-DNA interactions: sequence specificity and DNA bending for a simple ligand. *Nucleic Acids Res.* 17:6883–6892.

Feuerstein, B. G., N. Pattabiraman, and L. J. Marton. 1990. Molecular mechanics of the interactions of spermine with DNA: DNA bending as a result of ligand binding. *Nucleic Acids Res.* 18:1271–1282.

Fisher, D. E., L. A. Parent, and P. A. Sharp. 1992. Myc/Max and other helix-loop-helix/leucine zipper proteins bend DNA toward the minor groove. *Proc. Natl. Acad. Sci. USA.* 89:11779–11783.

Frank-Kamenetskii, M. D., V. V. Anshelevich, and A. V. Lukashin. 1987. Polyelectrolyte model of DNA. *Sov. Physics Uspekhi.* 151:595–618.

Fuoss, R. M., A. Katchalsky, and S. Lifson. 1951. The potential of an infinite rod-like molecule and the distribution of the counterions. *Proc. Natl. Acad. Sci. USA.* 37:579–589.

Gao, Y. G., H. Robinson, J. H. Van Boom, and A. H. J. Wang. 1995. Influence of counter-ions on the crystal structures of DNA decamers: binding of $[Co(NH3)6]^{3+}$ and Ba^{2+} to A-DNA. *Biophys. J.* 69:559–568.

Gessner, R. V., G. J. Quigley, A. H.-J. Wang, G. A. van der Marel, J. H. van Boom, and A. Rich. 1985. Structural basis for stabilization of Z-DNA by cobalt hexaammine and magnesium cations. *Biochemistry.* 24:237–240.

Goodsell, D. S., M. L. Kopka, D. Cascio, and R. E. Dickerson. 1993. Crystal structure of CATGGCCATG and its implications for A-tract bending models. *Proc. Natl. Acad. Sci. USA.* 90:2930–2934.

Gueron, M., and J.-P. Demaret. 1992. Polyelectrolyte theory. 4. Algebraic approximation for the Poisson-Boltzmann free energy of a cylinder. *J. Phys. Chem.* 96:7816–7820.

Hagerman, P. J. 1988. Flexibility of DNA. *Annu. Rev. Biophys. Biophys. Chem.* 17:265–286.

Hingerty, B. E., R. S. Brown, and A. Klug. 1982. Stabilization of the tertiary structure of yeast phenylalanine tRNA by $[Co(NH_3)_6]^{3+}$. X-ray evidence for hydrogen bonding to pairs of guanine bases in the major groove. *Biochim. Biophys. Acta.* 697:78–82.

Hingerty, B. E., R. H. Richie, T. L. Ferrel, and J. E. Turner. 1985. Dielectric effects in biopolymers: the theory of ionic saturation revisited. *Biopolymers.* 24:427–439.

Jayaram, B., and D. L. Beveridge. 1996. Modeling DNA in aqueous solutions: theoretical and computer simulation studies on the ion atmosphere of DNA. *Annu. Rev. Biophys. Biomol. Struct.* 25:367–394.

Kerppola, T. K., and T. Curran. 1991. DNA bending by Fos and Jun: the flexible hinge model. *Science.* 254:1210–1214.

Kopka, M. L., A. V. Fratini, H. R. Drew, and R. E. Dickerson. 1983. Ordered water structure around a B DNA dodecamer: a quantitative study. *J. Mol. Biol.* 163:129–146.

Lamm, G., L. Wong, and G. Pack. 1994. Monte Carlo and Poisson-Boltzmann calculations of the fraction of counterions bound to DNA. *Biopolymers.* 34:227–237.

Landau, L. D., and E. M. Lifshitz. 1976. Mechanics. Course in Theoretical Physics, Vol. 1. Pergamon, New York.

Lavery, R., H. Sklenar, and B. Pullman. 1986a. The flexibility of the nucleic acids: (III) the interaction of an aliphatic diamine, putrescine, with flexible B-DNA. *J. Biomol. Struct. Dyn.* 3:1015–1031.

Lavery, R., H. Sklenar, K. Zakrzewska, and B. Pullman. 1986b. The flexibility of the nucleic acids: (II) the calculation of internal energy and applications to mononucleotide repeat DNA. *J. Biomol. Struct. Dyn.* 3:989–1014.

Lebrun, A., and R. Lavery. 1996. Modelling extreme stretching of DNA. *Nucleic Acids Res.* 24:2260–2267.

Lebrun, A., Z. Shakked, and R. Lavery. 1997. Local DNA stretching mimics the distortion caused by the TATA box-binding protein. *Proc. Natl. Acad. Sci. USA.* 94:2993–2998.

Lukashin, A. V., D. B. Beglov, and M. D. Frank-Kamenetskii. 1991. Comparison of different approaches for calculation of polyelectrolyte free energy. *J. Biomol. Struct. Dyn.* 8:1113–1118.

Lyubartsev, A. P., and L. Nordenskiöld. 1995. Monte Carlo simulation study of ion distribution and osmotic pressure in hexagonally oriented DNA. *J. Phys. Chem.* 99:10373–10382.

Manning, G. S. 1978. The molecular theory of polyelectrolyte solutions with applications to the electrostatic properties of polynucleotides. *Q. Rev. Biophys.* 11:179–246.

Manning, G. S., K. K. Ebralidse, A. D. Mirzabekov, and A. Rich. 1989. An estimate of the extent of folding of nucleosomal DNA by laterally asymmetric neutralization of phosphate groups. *J. Biomol. Struct. Dyn.* 6:877–889.

Marquet, R., and C. Houssier. 1988. Different binding modes of spermine to A-T and G-C base pairs modulate the bending and stiffening of the DNA double helix. *J. Biomol. Struct. Dyn.* 6:235–246.

Marquet, R., C. Houssier, and E. Fredericq. 1985. An electro-optical study of the mechanisms of DNA condensation induced by spermine. *Biochim. Biophys. Acta.* 825:365–374.

Marquet, R., A. Wyart, and C. Houssier. 1987. Influence of DNA length on spermine-induced condensation. Importance of the bending and stiffening of DNA. *Biochim. Biophys. Acta.* 909:165–172.

Mondragon, A., and S. C. Harrison. 1991. The phage 434 Cro/O_R1 complex at 2.5 Å resolution. *J. Mol. Biol.* 219:321–334.

Nunn, C. M., and S. Neidle. 1996. The high resolution crystal structure of the DNA decamer d(AGGCATGCCT). *J. Mol. Biol.* 256:340–351.

Padmanabhan, S., V. M. Brushaber, C. F. Anderson, and M. T. Record, Jr. 1991. Relative affinities of divalent polyamines and of their *N*-methylated analogues for helical DNA determined by ^{23}Na NMR. *Biochemistry.* 30:7550–7559.

Paulsen, M. D., C. F. Anderson, and M. T. J. Record. 1988. Counterion exchange reaction on DNA: Monte Carlo and Poisson-Boltzmann analysis. *Biopolymers.* 27:1249–1265.

Plum, G. E., and V. A. Bloomfield. 1988. Equilibrium dialysis study of binding of hexammine cobalt(III) to DNA. *Biopolymers.* 27:1045–1051.

Porschke, D. 1984. Dynamics of DNA condensation. *Biochemistry.* 23: 4821–4828.

Porschke, D. 1986. Structure and dynamics of double helices in solution: modes of DNA bending. *J. Biomol. Struct. Dyn.* 4:373–389.

Pullman, B., R. Lavery, and A. Pullman. 1982. Two aspects of DNA polymorphism and microheterogeneity: molecular electrostatic potential and steric accessibility. *Eur. J. Biochem.* 124:229–238.

Quigley, G. J., M. M. Teeter, and A. Rich. 1978. Structural analysis of spermine and magnesium ion binding to yeast phenylalanine transfer RNA. *Proc. Natl. Acad. Sci. USA.* 75:64–68.

Randrianarivelo, M., K. Zakrzewska, and B. Pullman. 1989. Theoretical modeling of DNA-monocationic lexitropsin complexation: influence of ligand binding on DNA curvature. *J. Biomol. Struct. Dyn.* 6:769–779.

Robinson, H., and A. H. J. Wang. 1996. Neomycin, spermine and hexaamminecobalt(III) share common structural motifs in converting B- to A-DNA. *Nucleic Acids Res.* 24:676–682.

Rouzina, I., and V. A. Bloomfield. 1996. Macroion attraction due to electrostatic correlation between screening counterions. 1. Mobile surface-adsorbed ions and diffuse ion cloud. *J. Phys. Chem.* 100: 9977–9989.

Rouzina, I., and V. A. Bloomfield. 1997. Competitive electrostatic binding of charged ligands to polyelectrolytes—practical approach using the nonlinear Poisson-Boltzmann equation. *Biophys. Chem.* 64:139–155.

Rybenkov, V. V., A. V. Vologodskii, and N. R. Cozzarelli. 1997. The effect of ionic conditions on DNA helical repeat, effective diameter and free energy of supercoiling. *Nucleic Acids Res.* 25:1412–1418.

Sanghani, S. R., K. Zakrzewska, S. C. Harvey, and R. Lavery. 1996. Molecular modelling of $(A4T4NN)_n$ and $(T4A4NN)_n$: sequence elements responsible for curvature. *Nucleic Acids Res.* 24:1632–1637.

Schellman, J. A. 1974. Flexibility of DNA. *Biopolymers.* 13:217–226.

Schellman, J. A., and D. Stigter. 1977. Electrical double layer, zeta potential, and electrophoretic charge of double-stranded DNA. *Biopolymers.* 16:1415–1434.

Trifonov, E. N., R. K.-Z. Tan, and S. C. Harvey. 1987. Static persistence length of DNA. *In* Structure & Expression, Vol. 3, DNA Bending and Curvature. W. K. Olson, M. H. Sarma, R. H. Sarma, and M. Sundaralingam, editors. Adenine Press, Schenectady, NY.

Wang, M. D., H. Yin, R. Landick, J. Gelles, and S. M. Block. 1997. Stretching DNA with optical tweezers. *Biophys. J.* 72:1335–1346.

Wemmer, D. E., K. S. Srivenugopal, B. R. Reid, and D. R. Morris. 1985. Nuclear magnetic resonance studies of polyamine binding to a defined DNA sequence. *J. Mol. Biol.* 185:457–459.

Williams, L. D., C. A. Frederick, G. Ughetto, and A. Rich. 1990. Ternary interactions of spermine with DNA: 4′-epiadriamycin and other DNA: anthracycline complexes. *Nucleic Acids Res.* 18:5533–5541.

Xu, Q., S. R. B. Jampani, and W. H. Braunlin. 1993a. Rotational dynamics of hexaamminecobalt(III) bound to oligomeric DNA: correlation with cation-induced structural transitions. *Biochemistry.* 32:11754–11760.

Xu, Q., R. K. Shoemaker, and W. H. Braunlin. 1993b. Induction of B-A transitions of deoxyoligonucleotides by multivalent cations in dilute aqueous solution. *Biophys. J.* 65:1039–1049.

Zakrzewska, K., R. Lavery, and B. Pullman. 1987. A theoretical study of the sequence specificity in binding of lexitropsins to B-DNA. *J. Biomol. Struct. Dyn.* 4:833–843.

Zakrzewska, K., and B. Pullman. 1986. Spermine-nucleic acid interactions: a theoretical study. *Biopolymers.* 25:375–392.

Zhurkin, V. B. 1984. Sequence dependent anisotropic flexibility of B-DNA: a conformational study. *J. Biomol. Struct. Dyn.* 2:361–385.

Zhurkin, V. B., Y. P. Lysov, and V. I. Ivanov. 1978. Different families of double-stranded conformations of DNA as revealed by computer calculations. *Biopolymers.* 17:377–412.

Zhurkin, V. B., Y. P. Lysov, and V. I. Ivanov. 1980. Interaction of spermine with different forms of DNA. A conformational study. *Biopolymers.* 19:1415–1434.

Zimm, B. H., and M. Le Bret. 1983. Counter-ion condensation and system dimensionality. *J. Biomol. Struct. Dyn.* 1:461–471.